Cyclic Ketone Inhibitors of the Cysteine Protease Cathepsin K

Robert W. Marquis,*,† Yu Ru,† Jin Zeng,† Robert E. Lee Trout,† Stephen M. LoCastro,† Andrew D. Gribble,‡ Jason Witherington,‡ Ashley E. Fenwick,‡ Benedicte Garnier,‡ Thaddeus Tomaszek,§ David Tew,§ Mark E. Hemling,|| Chad J. Quinn,|| Ward W. Smith,⊥ Baoguang Zhao,⊥ Michael S. McQueney,# Cheryl A. Janson,# Karla D'Alessio,# and Daniel F. Veber†

Departments of Medicinal Chemistry (U.S.A.), Medicinal Chemistry (U.K.), Molecular Recognition, Physical and Structural Chemistry, Structural Biology, and Protein Biochemistry, GlaxoSmithKline, New Frontiers Science Park, Third Avenue, Harlow, Essex CM19 5AW, U.K., and 709 Swedeland Road, King of Prussia, Pennsylvania 19406

Received July 27, 2000

Cathepsin K (EC 3.4.22.38), a cysteine protease of the papain superfamily, is predominantly expressed in osteoclasts and has been postulated as a target for the treatment of osteoporosis. Crystallographic and structure−activity studies on a series of acyclic ketone-based inhibitors of cathepsin K have led to the design and identification of two series of cyclic ketone inhibitors. The mode of binding for four of these cyclic and acyclic inhibitors to cathepsin K is discussed and compared. All of the structures are consistent with addition of the active site thiol to the ketone of the inhibitors with the formation of a hemithioketal. Cocrystallization of the C-3 diastereomeric 3-amidotetrahydrofuran-4-one analogue **16** with cathepsin K showed the inhibitor to occupy the unprimed side of the active site with the 3*S* diastereomer preferred. This C-3 stereochemical preference is in contrast to the X-ray cocrystal structures of the 3-amidopyrrolidin-4-one inhibitors **29** and **33** which show these inhibitors to prefer binding of the 3*R* diastereomer. The 3-amidopyrrolidin-4-one inhibitors were bound in the active site of the enzyme in two alternate directions. Epimerization issues associated with the labile α-amino ketone diastereomeric center contained within these inhibitor classes has proven to limit their utility despite promising pharmacokinetics displayed in both series of compounds.

Introduction

The proteolytic processing of endogenous peptide substrates by cysteine proteases has been implicated in the pathology of a wide variety of diseases.[1] These diseases include inflammation,[2] tumor progression,[3] parasitic infections,[4] and osteoporosis.[5] Cathepsin K (EC 3.4.22.38), a 24-kDa cysteine protease of the papain superfamily, is selectively and abundantly expressed within osteoclasts.[6] Upon expression, this protease is secreted from the osteoclast into the resorption pit where it degrades the protein matrix of bone. The osteoclast-selective expression of cathepsin K suggests that this enzyme may play a crucial role in the degradative phase of the remodeling of the bone matrix. As such, selective inhibition of this enzyme could prove to be an effective strategy for the treatment of diseases such as osteoporosis, which is characterized by an imbalance between the formation and resorption of the bone matrix. Several recently published studies support this hypothesis. First, Gelb and Johnson have shown that mutations in the gene which encodes for cathepsin K are associated with a rare autosomal disorder of bone remodeling known as pycnodysostosis.[7] This disease is characterized by short stature, dwarfism, high bone fracture rates, and osteosclerosis. Second, through the use of an antisense oligonucelotide, Yamamura and coworkers have inhibited osteoclast bone resorption in a dose-dependent manner.[8] Finally, two groups have independently generated cathepsin K-deficient mice which were viable but displayed a distinct osteopetrotic phenotype.[9]

Two of the key issues in the development of therapeutically useful inhibitors of proteases involve the mechanism of protease inhibition as well as the optimization of structural features and physiochemical properties which may limit their oral bioavailabilty.

Cysteine protease inhibitors may be broadly divided into two classes.[10] The first are a series of active site titrants whose mechanism for inhibition is to permanently modify the target protease via an irreversible alkylation of the active site cysteine. Notable examples of this inhibitor class include the naturally derived epoxide E-64,[11] the (acyloxy)methyl ketone quiescent affinity labels,[12] peptidyl vinyl sulfones,[13] and α,β-unsaturated esters.[14] The second class of inhibitor is based on the formation of a covalent, yet fully reversible, transition-state intermediate with the thiol of the active site cysteine residue. Inhibitors in this series include peptide aldehydes,[15] cyclopropenones,[16] peptide nitriles,[17] α-keto amides,[18] and diamino ketones.[19]

Our efforts have focused on the development of reversible inhibitors of cathepsin K. In a disease such as osteoporosis, which would most likely require chronic administration of a therapeutic agent, reversible inhibition may avoid immunological responses which are associated with the permanent, covalent modification of proteins.[20] We have recently disclosed a series of

* To whom correspondence should be addressed. Phone: 1-610-270-6570. Fax: 1-610-270-4451. E-mail: Robert_W_Marquis@sbphrd.com.
† Department of Medicinal Chemistry (U.S.A.).
‡ Department of Medicinal Chemistry (U.K.).
§ Department of Molecular Recognition.
|| Department of Physical and Structural Chemistry.
⊥ Department of Structural Biology.
Department of Protein Biochemistry.

10.1021/jm000320t CCC: $20.00
Published on Web 01/24/2001

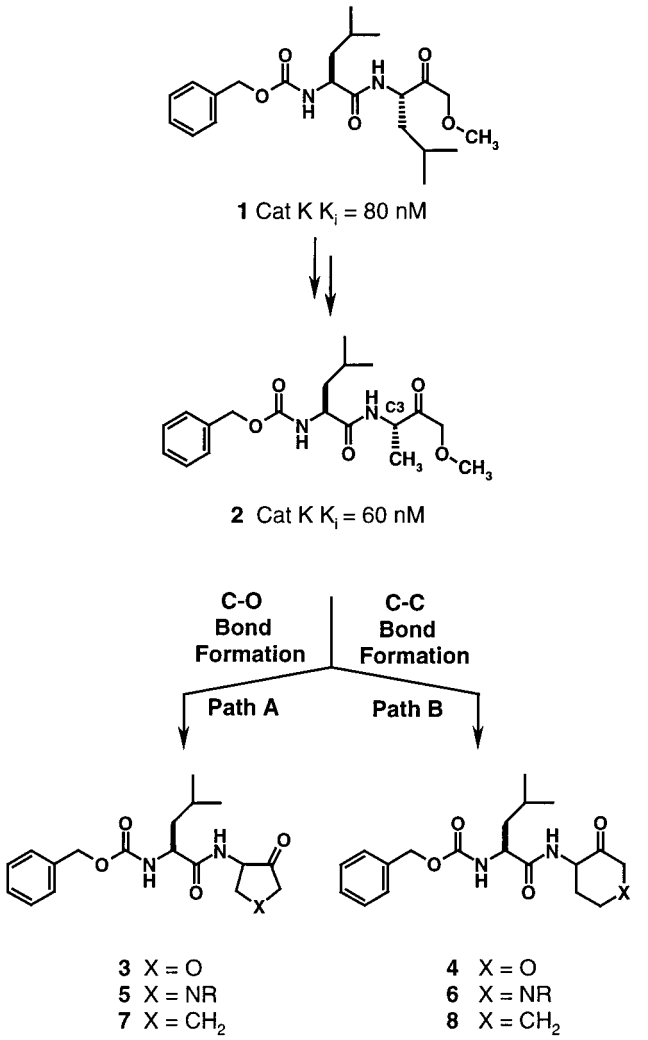

Figure 1. C−O and C−C bond formation of acyclic alkoxymethyl ketone **2** to provide 3-amidotetrahydrofuran-4-one and 4-amidotetrahydropyran-3-one inhibitors **3** and **4**. Substitution of nitrogen and carbon for oxygen provides analogues **5**−**8**.

potent, reversible alkoxymethyl ketone inhibitors of cathepsin K (**1**; Figure 1)[21] which were based upon the alkoxymethyl ketone template originally developed by Szelke and co-workers for the inhibition of the serine protease thrombin.[22] While examining substitutions of the P_1 amino acid of the lead methoxymethyl ketone inhibitor **1** (cathepsin K $K_{i,app}$ = 80 nM; Figure 1)[23] we had shown that the isobutyl moiety **1** could be replaced by a methyl group to afford inhibitor **2** (cathepsin K $K_{i,app}$ = 60 nM) without loss of inhibitory potency. In the course of designing cyclic conformational constraints it became clear that simple incorporation of ketone-based ring systems into this acyclic template could lead to potent inhibitors. As outlined in Figure 1, cyclization of inhibitor **2** along path A by the formation of a carbon−oxygen bond between the alanine methyl group and the oxygen of the methyl ether generates the 3-amidotetrahydrofuran-4-one **3**.[24] Alternatively, cyclization along path B by the formation of a carbon−carbon bond between the alanine methyl group and the methyl ether carbon provides the 4-amidotetrahydropyran-3-one derivative **4**. Substitution of nitrogen for the oxygen of inhibitors **3** and **4** provides the previously reported 3-amidopyrrolidin-4-one- and 4-amidopiperidin-3-one-based analogues **5** and **6**.[25] Although the pyrrolidinone

Scheme 1. Synthesis of 3-Amidotetrahydrofuran-4-one and 4-Amidotetrahydropyran-3-one Inhibitors[a]

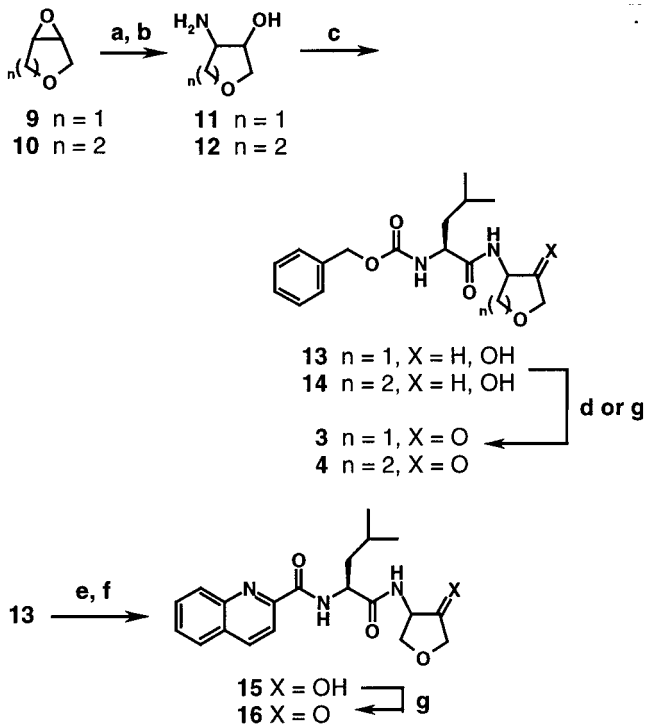

[a] Reagents and conditions: (a) NaN_3, NH_4Cl, CH_3OH, H_2O; (b) H_2, 10% Pd/C, CH_3OH; (c) Cbz-leucine, EDC, CH_2Cl_2; (d) $(COCl)_2$, DMSO, TEA; (e) 10% Pd/C, H_2, EtOAc; (f) quinoline-2-carboxylic acid, EDC; (g) SO_3−pyridine, TEA, DMSO.

and piperidinone ring systems followed conceptually from the furanone and pyranone systems, synthetic expedience led first to the nitrogen-based ketones which have been previously reported in this Journal.[25] Substitution of the oxygen or nitrogen in the heterocyclic rings of these templates with a methylene group provides the carbocyclic analogues **7** and **8**. These carbocycles were prepared in order to determine the role the heteroatom plays in modulating the electrophilicity of the carbonyl group contained within the cyclic inhibitor templates described herein.

Synthesis Chemistry

The syntheses of the 3-amidotetrahydrofuran-4-one and 4-amidotetrahydropyran-3-one inhibitors **3**, **4**, and **16** are detailed in Scheme 1. Opening of the commercially available 3,4-epoxytetrahydrofuran (**9**) with sodium azide followed by reduction of the intermediate azido alcohol provided the amino alcohol **11**. Acylation of **11** with Cbz-leucine in the presence of 1-[3-(dimethylamino)propyl]-3-ethylcarbodiimide hydrochloride (EDC) provided alcohol intermediate **13** which was oxidized to provide ketone **3** as a mixture of diastereomers. In a similar fashion, opening of the epoxide **10** with sodium azide followed by reduction using hydrogen in the presence of 10% palladium on carbon provided the amino alcohol **12** along with approximately 20% of the regioisomeric amino alcohol (not shown).[26] The undesired regioisomer was separated by column chromatography at a later stage of the synthesis. Acylation of **12** with Cbz-leucine in the presence of EDC provided alcohol **14** which on Swern oxidation provided the ketone **4** as a mixture of diastereomers. Hydrogenolysis

Scheme 2. Synthesis of Pyrrolidinone and Piperidinone Inhibitors **22**−**29**[a]

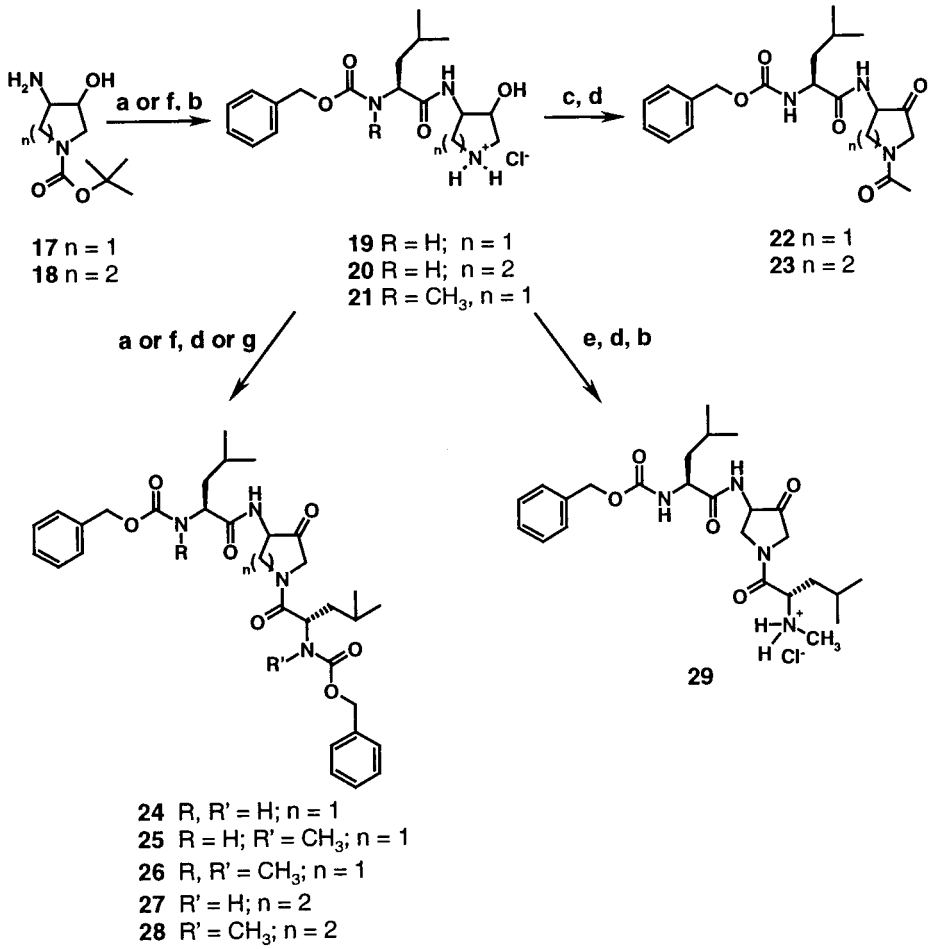

[a] Reagents and conditions: (a) Cbz-leucine, EDC, HOBt, CH_2Cl_2; (b) HCl, EtOAc; (c) AcCl, DIPEA, CH_2Cl_2 or HOAc, EDC, CH_2Cl_2; (d) $(COCl)_2$, DMSO, TEA, CH_2Cl_2; (e) *N*-Boc-*N*-methylleucine, EDC, CH_2Cl_2; (f) *N*-Cbz-*N*-methylleucine, EDC, HOBt, CH_2Cl_2; (g) Jone's reagent, acetone.

of the Cbz group of intermediate **13** followed by acylation of the resulting amine with quinoline-2-carboxylic acid provided the alcohol intermediate **15** which was oxidized under Parikh conditions[27] to provide **16** as a 1:1 mixture of diastereomers.

The syntheses of the pyrrolidinone and piperidinone inhibitors **22**−**29** are detailed in Scheme 2 and follow the general procedures described in our earlier communication of a portion of this work.[25] Acylation of the amino alcohols **17**[28]and **18**[29] with either Cbz-leucine or *N*-methyl-Cbz-leucine in the presence of EDC followed by removal of the *tert*-butoxycarbonyl protecting group under acidic conditions provided the amine salts **19**−**21**. Acylation of the amine salt **19** with acetic acid in the presence of EDC followed by Swern oxidation of the resulting alcohol provided **22**. Alternatively, acylation of **20** with acetyl chloride and oxidation gave **23**. Inhibitors **24**−**28** were synthesized by the acylation of amine salts **19**−**21** with either Cbz-leucine or *N*-Cbz-*N*-methylleucine followed by oxidation of the intermediate alcohols. Alternatively, acylation of amine salt **19** with Boc-*N*-methylleucine followed by oxidation of the intermediate alcohol and removal of the *tert*-butoxycarbonyl protecting group under acidic conditions provided inhibitor **29**.

Inhibitor **33** was synthesized beginning with the EDC-mediated acylation of amino alcohol **30** with *N*-Boc-leucine (Scheme 3). Hydrogenolysis of the benzyloxycarbonyl protecting group provided amino alcohol intermediate **31**. Reductive amination of **31** with Cbz-leucinal in the presence of sodium triacetoxyborohydride and subsequent removal of the N-Boc protecting group gave the intermediate amine salt **32**. Coupling of **32** with quinoline-7-carboxylic acid followed by SO_3−pyridine oxidation of the resulting alcohol provided the diastereomeric ketones **33**.

The syntheses of the carbocyclic analogues **7** and **8** are shown in Scheme 4. Acylation of the known amino alcohols **34** and **35** with Cbz-leucine provided alcohols **36** and **37**. Parikh oxidation of these alcohols provided the ketone derivatives **7** and **8** as mixtures of diastereomers.

Results and Discussion

Cathepsin K inhibition and selectivity data versus human cathepsins B, S, and L are shown in Table 1.[30] Cyclization of the alkoxymethyl ketone inhibitor **2** produced the diastereomeric 3-amidotetrahydrofuran-4-one and the 4-amidotetrahydropyran-3-one analogues **3** and **4** which resulted in only a slight loss of activity when tested as a 1:1 mixture of diastereomers. Both **3** and **4** are selective inhibitors of cathepsin K versus cathepsins B and L but were less selective for cathepsin K over cathepsin S. The alcohol precursors **13** and **14**

Scheme 3. Synthesis of Pyrrolidinone Inhibitor **33**[a]

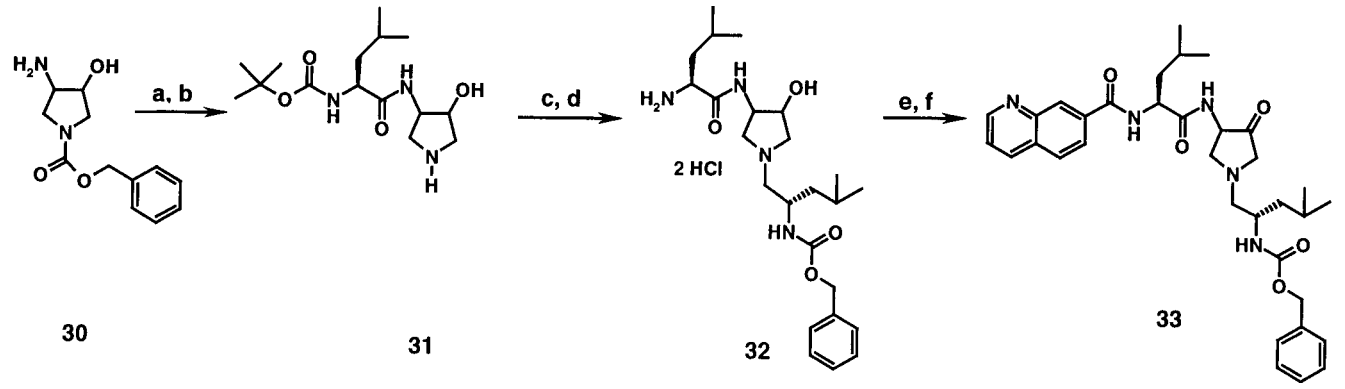

[a] Reagents and conditions: (a) *N*-Boc-leucine, EDC; (b) H_2, 10% Pd/C, CH_3OH; (c) Cbz-leucinal, $NaBH(OAc)_3$, CH_2Cl_2; (d) HCl, EtOAc, CH_3OH; (e) quinoline-7-carboxylic acid, EDC, HOBt; (f) SO_3−pyridine, TEA, DMSO.

Scheme 4. Synthesis of Carbocyclic Inhibitors **7** and **8**[a]

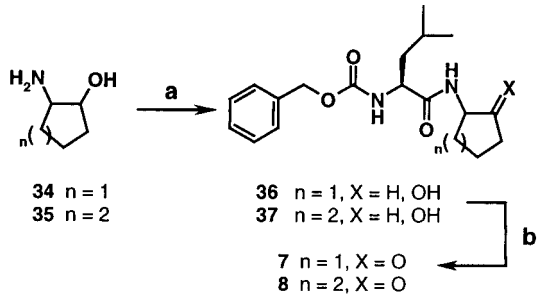

[a] Reagents and conditions: (a) Cbz-leucine, EDC; (b) SO_3−pyridine, TEA, DMSO.

Table 1. Cathepsin K, B, S, and L Inhibition Data[a−c]

	$K_{i,app}$ (nM)			
inhibitor	cathepsin K	cathepsin B	cathepsin S	cathepsin L
2	60	>1000		513
3	140	>10000	310	2600
4	150	>10000	530	850
7	>10000	>10000	>10000	>10000
8	>10000	>10000	>10000	>10000
13	>1000		>1000	>1000
14	>1000		>1000	>1000
16	44	7800	1100	250
22	250		480	580
23	230			
24	2.3	>1000	90	39
25	0.6			
26	180	2600	51	49
27	2.6	440	8.0	16
28	1.9			
29	77	7300	290	400
33	1.6	46		

[a] With the exception of inhibitor **2**, all compounds were tested as mixtures of diastereomers. [b] See ref 30 for enzyme assay conditions. [c] Average standard errors for $K_{i,app}$ values were 3−10%.

were significantly less active than the corresponding ketone derivatives **3** and **4** with $K_{i,app}$'s > 1000 nM when tested as a mixture of diastereomers. This result is in agreement with the transition state mechanism of inhibition for ketone-based inhibitors.[31] The Lineweaver−Burk plot of **3** displays a 1/*v* axis intercept which is constant with increasing inhibitor concentration, indicative of competitive inhibition (see Supporting Information). Competitive inhibition was also observed for **4**. Neither compound displayed time-dependent inhibition over a 30-min progress curve analysis. Ketones **3** and **4** were also shown to be reversible inhibitors of cathepsin K. In separate experiments, incubation of **3** and **4** with cathepsin K for 2 h followed by LC−MS analysis of the protein/inhibitor mixture showed no covalent modification of the protein. Preincubation of excess of **3** or **4** with cathepsin K for 2 h followed by addition of the fluorescent substrate Z-Phe-Arg-AMC revealed no loss of enzyme activity. This experiment provides additional evidence for the reversible mechanism of inhibition of these compounds. The quinoline-2-carboxamide **16** is 4 times as potent as analogue **3** with a $K_{i,app}$ = 44 nM when tested as a 1:1 mixture of diastereomers.[32] X-ray crystallographic analysis of the inhibitor **16**/cathepsin K complex at 2.5 Å resolution shows the inhibitor oriented on the unprimed side of the active site (Figure 2). The leucine is seen bound within the hydrophobic S_2 pocket formed by residues Leu 160, Ala 134, and Met 68 of the protein. The quinoline group is bound in the S_3 binding pocket forming a $\pi-\pi$ stack with Tyr 67.[33] The direction of binding for this inhibitor is likely to be a result of both the π-stacking interaction formed between the quinoline carboxamide and Tyr 67 as well as the preferred specificity of the S_2 binding pocket of cathepsin K for leucine.[13b] The X-ray cocrystal structure is consistent with the formation of a hemithioketal between Cys 25 of cathepsin K and the carbonyl group of the tetrahydrofuran-3-one, confirming our initial hypothesis for the design of reversible, transition-state inhibitors of cysteine proteases. The oxygen of the hemithioketal is stabilized by two hydrogen bonds formed within the oxyanion hole of the enzyme with the $C(O)NH_2$ group of Gln 19 as well as the NH of Cys 25. The stereochemistry of the C-3 diastereomeric center is consistent with the *S* configuration. Since the rate of epimerization of the C-3 chiral center is rapid relative to the rate of crystallization, this stereochemical preference may be a reflection of the more potent of the two diastereomers or may be a result of crystal packing forces. Assuming that the *S* diastereomer of **16** has formed the initial complex with cathepsin K, then the active site cysteine has added to the diastereotopically more hindered *si* face of the ketone. Two hydrogen bonds were observed between Gly 66 of the enzyme with the C-3 leucinamide portion of the inhibitor. The C-2 methylene group of the tetrahydrofuran-3-one ring is directed out toward solvent with no apparent interactions with the protein. The orientation of the C-2 methylene group toward solvent suggests that this portion of the molecule may serve as a suitable position

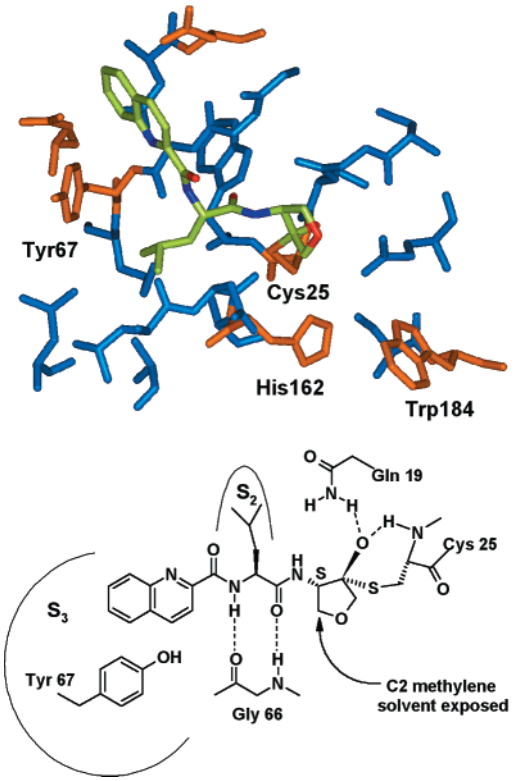

Figure 2. The 2.5 Å X-ray cocrystal structure of inhibitor **16** (yellow) seen bound within the active site of cathepsin K (blue and orange). The inhibitor is oriented on the unprimed side of the active site with the isobutyl group of the inhibitor bound within the hydrophobic S_2 binding pocket The extended π-aromatic of the quinoline moiety is seen bound in the S_3 pocket of the active site. A tetrahedral hemithioketal is formed between the ketone carbonyl of the inhibitor and the active site Cys 25 of cathepsin K. The thiol group of Cys 25 has added to the sterically more congested *si* face of the carbonyl group of **16**. The inhibitor has crystallized within the enzyme active site with the *S* stereochemistry at the C-3 stereocenter.

from which to optimize the physiochemical properties of these inhibitors which may play a role in determining their pharmacokinetic behavior.

The direction of binding for inhibitor **16** in the active site of cathepsin K is opposite to the previously published X-ray cocrystal structure of the weakly time-dependent acyclic *n*-propyloxymethyl ketone inhibitor **38** ($K_{inact/I}$ = 4100 M^{-1} s^{-1}; Figure 3).[21] In this X-ray cocrystal structure, **38** was oriented on the primed side of the active site with the isobutyl groups bound in the S_1' and S_2' pockets of the protein. The phenyl moiety of the benzyloxycarbonyl group was seen bound in the S_3' pocket forming an edge−face interaction with Trp 184. This edge−face aromatic interaction between the phenyl moiety of the inhibitor and the indole of Trp 184 may be the most critical for determining the direction of binding for this inhibitor. The N-H of Trp 184 forms a hydrogen bond with the urethane carbonyl of the inhibitor, while the amide carbonyl of **38** forms a hydrogen bond with the N-H group of His 162. The X-ray cocrystal structure was consistent with the addition of the thiol group of the active site Cys 25 to the carbonyl of **38**, forming a hemithioketal. The oxygen of the hemithioketal is stabilized in the oxyanion hole by hydrogen bonds to the Cys 25 NH and the $H_2NC(O)$ of Gln 19. Here, the thiol group of the active site cysteine

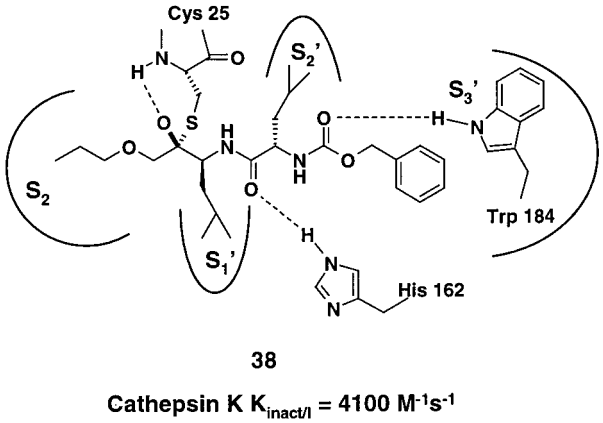

Figure 3. Schematic representation of the 2.5 Å X-ray cocrystal structure of the inhibitor **38** bound within the active site of cathepsin K (see ref 21).

has added to the *re* face of the carbonyl group in a Felkin−Anh manner, opposite to the bulky P_1' isobutyl group. The *n*-propyl alkyl side chain was oriented on the unprimed side of the active site partially penetrating the hydrophobic S_2 binding pocket.

Replacement of the ring oxygen atom of **3** and **4** with an *N*-acetyl moiety provided **22** and **23** which were 250 and 230 nM inhibitors of cathespin K, respectively (again tested as a 1:1 mixture of diastereomers). Inhibitor **23** showed a 2-fold selectivity for cathepsin K versus cathepsins L and S. Replacement of the *N*-acetyl group with Cbz-leucine in order to introduce additional binding elements which would permit access to both sides of the active site provided analogues **24** and **27** which are 2.3 and 2.6 nM inhibitors of cathepsin K, respectively. The approximately 100-fold increase in potency upon incorporation of the C-3 leucinamide reflects the additional binding energies associated with the inhibitor occupying the S_3 and S_3' binding pockets of the active site of the protein. Inhibitor **24** showed good selectivity for cathepsin K over cathepsins B, L, and S, while **27** was somewhat less selective for cathepsin K versus cathepsins L and S. These cyclic diamino ketones were also characterized as competitive, reversible inhibitors of cathepsin K. Incubation of **24** or **27** with cathepsin K followed by LC−MS analysis showed that there had been no irreversible covalent modification of the enzyme. The *N*-methylated analogues **25** and **28** were also potent inhibitors of cathepsin K with $K_{i,app}$'s of 0.6 and 1.9 nM, respectively. *N*-Methylation has also served to elucidate the relative importance of the hydrogen bond which is formed between the inhibitor and the amide carbonyl of Gly 66 of the protein. The bis-*N*-methyl analogue **26** was significantly less potent than **25** indicating that the methylation of the C-3 leucinamide has either eliminated a critical hydrogen bond between the inhibitor and the enzyme and/or imparted a highly unfavorable conformation of the urethane which precluded effective inhibitor binding. Removal of the benzyloxycarbonyl moiety from **25** provided **29** which was a 77 nM inhibitor of cathepsin K. The loss in activity of **29** relative to **25** highlights the role of the carbonylbenzyloxy moiety for potent inhibition. The 2.4 Å resolution X-ray cocrystal structure of **29** shows that this inhibitor spans both the primed and unprimed sides of the active site (Figure 4). The direction of binding of inhibitor **29** is the same

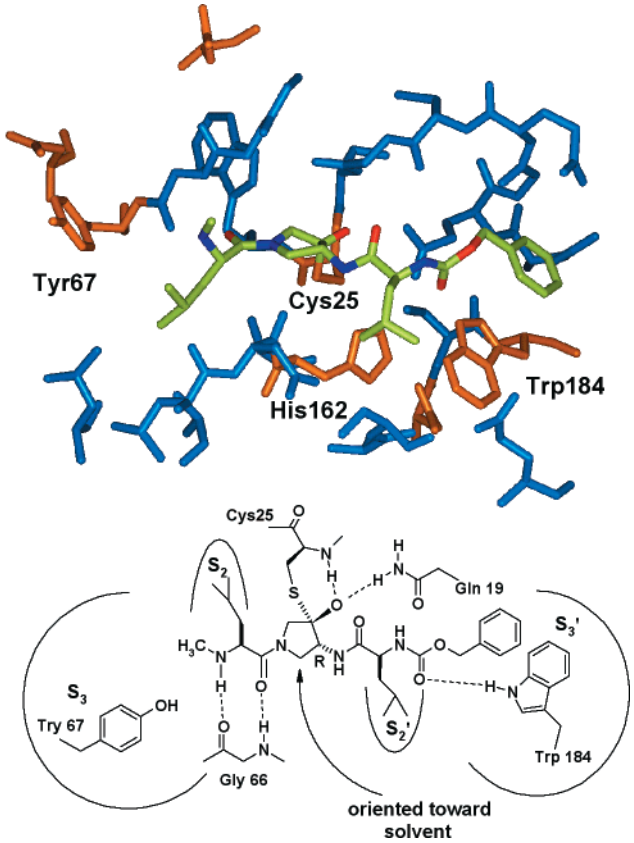

Figure 4. The 2.4 Å X-ray cocrystal structure of inhibitor **29** (yellow) seen bound within the active site of cathepsin K (blue and orange). The inhibitor spans S_2 to S_3' of the active site. A tetrahedral hemithioketal is formed between the ketone carbonyl of the inhibitor and the active site Cys 25 of cathepsin K with the thiol moiety adding from the more hindered *si* face of the carbonyl group. The inhibitor has crystallized within the enzyme active site with the *R* stereochemistry at the C-3 diastereomeric center.

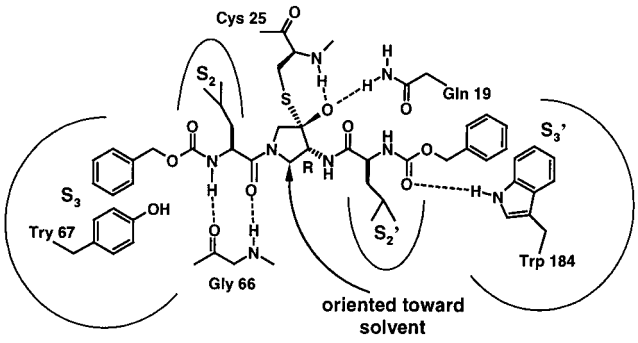

Figure 5. Schematic representation of the 2.3 Å resolution X-ray cocrystal structure of inhibitor **24** bound within the active site of cathepsin K (see ref 25). The inhibitor spans the active site of the protein with the thiol of Cys 25 adding to the sterically more congested *si* face of the carbonyl group of the inhibitor. The inhibitor has crystallized within the active site with the *R* stereochemistry at the C-3 chiral center of the pyrrolidinone ring.

as that of the previously published cocrystal structure of inhibitor **24** (see Figure 5).[25] In both structures the N-1 tertiary amide of the pyrrolidinone ring is bound on the unprimed side while the C-3 leucinamide is seen bound on the primed side of the active site. The X-ray cocrystal structure of **29** is consistent with the formation of a covalent bond between the ketone carbonyl of the inhibitor and the thiol group of Cys 25 of the protein. Here again, the oxygen of the hemithioketal is stabilized within the oxyanion hole by two hydrogen bonds with the backbone N-H of Cys 25 and the $C(O)NH_2$ of Gln 19. The inhibitors in the cocrystal structures of both **24** and **29** have crystallized within the active site with the R configuration of the labile C-3 stereocenter. As in the case of the inhibitor **16**/cathepsin K complex, this stereochemical preference for the *R* diastereomer may be a reflection of the more active of the two diastereomers or may be a result of crystal packing forces. The sulfur nucleophile of Cys 25 has added to the sterically more congested *si* face of **29**. The S_3 pocket of the inhibitor **29**/cathepsin K complex is vacant, while the S_2 pocket is occupied by the isobutyl group. The C-2 methylene group of the pyrrolidinone ring in the crystal structures of both **24** and **29** is oriented away from the protein backbone toward solvent making no significant contacts with the protein. As in the X-ray cocrystal structure of furanone derivative **16**, the orientation of the C-2 methylene group toward solvent suggests that this position may be used to alter the pharmacokinetic properties of these inhibitors or to slow the rate of enolization of the C-3 methine hydrogen. The isobutyl group of the C-3 leucinamide is bound in the S_2' pocket with the aryl group of the carbonylbenzyloxy group located in the S_3' pocket forming a $\pi-\pi$ stacking interaction with Trp 184. Again, we believe that it is this interaction which has dominated the direction of binding for this inhibitor.

Analogue **33**, in which a methylene group has replaced the N-1 tertiary amide and a quinoline-7-carboxamide has replaced the carbonylbenzyloxy group, is as potent as the parent cyclic diamino ketone **24** with a $K_{i,app}$ = 1.6 nM as a diastereomeric mixture. These changes have served to reduce the peptidic nature of these inhibitors while also increasing their overall aqueous solubility. As seen in Figure 6, the 1.9 Å resolution cocrystal structure of analogue **33**/cathepsin K reveals that this inhibitor again spans both sides of the active site. In contrast to the direction of binding of inhibitors **24** and **29**, analogue **33** binds in the opposite direction, with the N-1 tertiary amine of the pyrrolidinone ring oriented on the primed side of the active site and the C-3 leucinamide on the unprimed side. The C-3 diastereomeric center with the *R* configuration has crystallized within the active site of the protein. The active site cysteine has added to sterically more accessible *re* face of the ketone, opposite to the C-3 leucinamide moiety. The quinoline-7-carboxamide is bound in the S_3 pocket of cathepsin K, forming an edge−face electrostatic interaction with Tyr 67. The isobutyl moiety of the C-3 leucinamide lies within the S_2 pocket. On the primed side of the active site the isobutyl group of the N-1 tertiary amine is bound within the S_2' pocket with the phenyl of the Cbz group in the S_3' pocket forming a $\pi-\pi$ stack with Trp 184. The orientation of binding for **33** is likely a result of the preferred interactions of the phenyl moiety of the inhibitor with the S_3' tryptophan of the protein and the extended π aromatic group of the quinoline-7-carboxamide with Tyr 67 of the S_3 binding pocket. In this example, the S_2 binding pocket may be irrelevant to the direction of inhibitor binding due to the presence of two isobutyl groups in the inhibitor.

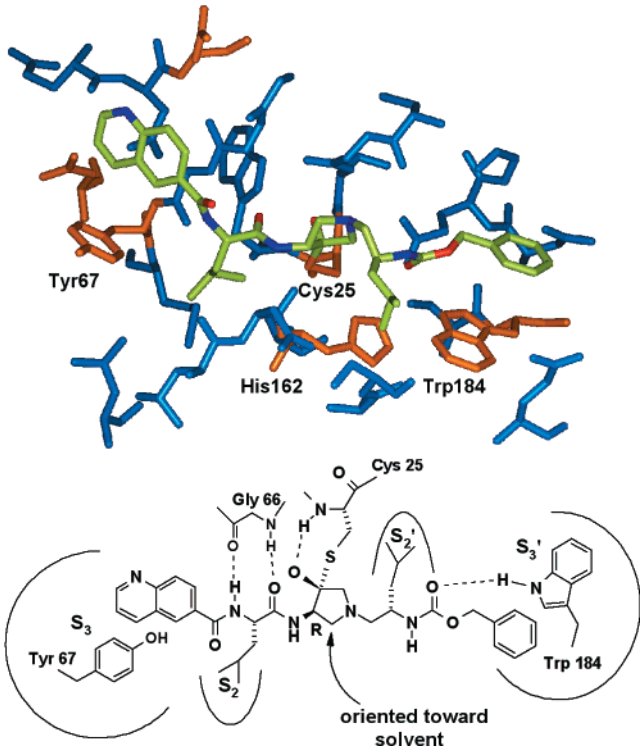

Figure 6. The 1.9 Å X-ray cocrystal structure of inhibitor **33** (yellow) seen bound within the active site of cathepsin K (blue and orange). The inhibitor is bound within the S_3 to S_3' pockets of the active site. A tetrahedral hemithioketal is formed between the ketone carbonyl of the inhibitor and the active site Cys 25 of cathepsin K with addition of the thiol from the sterically more accessible *re* face of the ketone. The inhibitor has crystallized within the enzyme active site with the *R* stereochemistry at the α-amino carbon stereocenter.

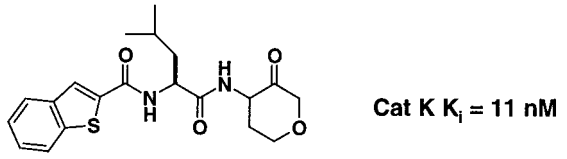

39 Cat K K_i = 11 nM

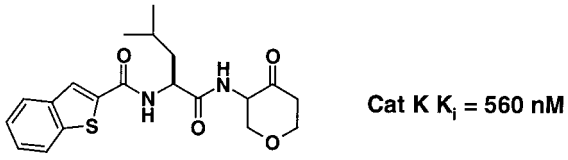

40 Cat K K_i = 560 nM

Figure 7. Effect of positioning of the heteroatom on inhibitor potencies.

Removal of the electron-withdrawing oxygen or nitrogen heteroatoms from the cyclic ketone templates provided the carbocyclic ketones **7** and **8** which were not active up to a concentration of 10 μM when tested against cathepsins K, B, L, and S. Analogues **39** and **40** were evaluated as inhibitors of cathepsin K in order to determine the effect that the positioning of the heteroatom within a cyclic framework has on inhibitor potency. As shown in Figure 7, the 4-amidotetrahydropyran-3-one **39** is an 11 nM inhibitor of cathepsin K when tested as a mixture of diastereomers. Analogue **40**, in which the oxygen is now positioned γ to the ketone, is a 560 nM inhibitor. This loss in inhibitor potency relative to the positioning of the heteroatom within the cyclic ketone framework reveals the dramatic difference between a through-bond effect and a through-space electrostatic effect in altering the reactivity of the ketone carbonyl group of these inhibitors.[34] These results highlight the essential requirement of these heteroatoms for the potent inhibition of cysteine proteases by cyclic ketone-based inhibitors.

Having established the cyclic ether and the cyclic amine classes of compounds as potent, reversible inhibitors of cathepsin K, the pharmacokinetics of several analogues in each of these series where evaluated in order to determine if the introduction of a conformational constraint has improved the bioavailability of these compounds relative to their acyclic counterparts. Their pharmacokinetic behavior was profiled in the rat as multicomponent mixtures utilizing LC−MS−MS analysis following modified protocols described by Shaffer and co-workers.[35] Several analogues from each class displayed promising pharmacokinetics in the rat. However due to the facile epimerization of the α-amino ketone chiral center, these compounds were unsuitable for further development or for full pharmacokinetic evaluation of the active diastereomer.

Conclusions

In this paper we have disclosed a new series of 3-amidotetrahydrofuran-4-one- and 4-amidotetrahydropyran-3-one-based inhibitors of the cysteine protease cathepsin K. These inhibitors were characterized as reversible and competitive. The binding of one of these cyclic inhibitors was demonstrated by X-ray cocrystallization with the protein, to bind on the unprimed side of the active site. This mode of binding was opposite to the orientation of an acyclic analogue which was seen bound on the primed side of the active site. X-ray crystallographic analysis of two 3-amidopyrrolidin-4-one-based inhibitors reveals these analogues to bind in opposite directions in the active site. The X-ray crystallographic analysis of several protein/inhibitor complexes was instrumental in delineating the contribution of the electrostatic interactions which determine the direction of binding for both the cyclic ether and the cyclic diamino ketone inhibitor classes. Furthermore, all the cocrystal structures presented herein revealed that the C-2 methylene group in all of the bound inhibitors is oriented away from the protein toward solvent. This observation suggests that this group may be used to attenuate the rate of epimerization of this class of cyclic ketone inhibitors. The introduction of a conformational constraint was seen to provide potent inhibitors which displayed promising, yet inconclusive, pharmacokinetics.

Experimental Procedures

General. All materials and reagents were used as supplied. Nuclear magnetic resonance spectra were recorded at 400 MHz using a Bruker AC 400 spectrometer. Chemical shifts are reported in parts per million (δ). Mass spectra were taken on either VG 70 FE, PE Sciex API III, or VG ZAB HF instruments, using electrospray ionization (ESI) techniques. Elemental analyses were obtained using a Perkin-Elmer 240C elemental analyzer. Reactions were monitored by TLC analysis using Analtech silica gel GF or E. Merck silica gel 60 F-254 thin layer plates. Flash chromatography was carried out on E. Merck Kieselgel 60 (230−400 mesh) silica gel.

***trans*-4-Amino-3-hydroxytetrahydrofuran (11).** 3,4-Epoxytetrahydrofuran (9 g, 105 mmol) was added to a stirred solution of sodium azide (27 g, 415 mmol) and ammonium chloride (9 g, 159 mmol) in aqueous methanol (95%, 200 mL). The reaction was heated to 75 °C and stirred for 20 h. The reaction was cooled, filtered and evaporated under reduced pressure. The residue was diluted with water and extracted with ethyl acetate, dried and evaporated under reduced pressure to afford 10g (74%) of *trans*-4-azido-3-hydroxytetrahydrofuran as a clear oil: ^{1}H NMR (400 MHz, $CDCl_3$) δ 4.32 (m, 1H), 4.09 (dd, 1H, J = 4.8, 9.9 Hz), 3.99 (dd, 1H, J = 4.3, 10.1 Hz), 3.94 (m, 1H), 3.81 (dd, J = 2.1, 9.9 Hz), 3.73 (dd, 1H, J = 1.8, 10.1 Hz), 2.72 (d, 1H, J = 4.6 Hz).

To a solution of *trans*-4-azido-3-hydroxytetrahydrofuran (13.2 g, 102 mmol) in methanol (100 mL) was added 10% palladium on charcoal (2 g). The reaction was stirred under an atmosphere of hydrogen overnight whereupon it was filtered and concentrated to give 10.2 g of **11** as a brown solid. This material was of sufficient purity to carry on to the next step with no further purification.

[(*S*)-1-((3*R*,*S*),(4*R*,*S*)-4-Hydroxytetrahydrofuran-3-ylcarbamoyl)-3-methylbutyl]carbamic Acid Benzyl Ester (13). To a solution of amino alcohol **11** (1.0 g, 9.7 mmol) in CH_2Cl_2 (20 mL) were added Cbz-leucine (2.83 g, 10.7 mmol) and EDC (2.83 g, 21.3 mmol). The reaction was maintained at room temperature for 2 h whereupon it was concentrated. The residue was dissolved in ethyl acetate and washed with 1 N HCl, saturated $NaHCO_3$, brine, dried ($MgSO_4$), filtered and concentrated. Column chromatography (2:1 hexanes:ethyl acetate) of the residue provided 1.7 g (50%) of **13** as a white powder: ^{1}H NMR (400 MHz, DMSO-d_6, reported as a mixture of diastereomers) δ 8.08 (app d, 1H), 7.34 (m, 5H), 5.24 (br s, 1H), 5.01 (app s, 2H), 4.03−3.78 (m, 5H), 3.49−3.32 (m, 3H), 1.58−1.33 (m, 3H), 0.87−0.83 (m, 6H); MS(ESI) 351.1 (M + H)$^+$, 372.6 (M + Na)$^+$. Anal. ($C_{18}H_{26}N_2O_5$·0.15EtOAc) C, H, O.

[(*S*)-1-((3*R*,*S*)-4-Oxotetrahydrofuran-3-ylcarbamoyl)-3-methylbutyl]carbamic Acid Benzyl Ester (3). To a −78 °C solution of oxalyl chloride (0.11 mL, 1.3 mmol) in CH_2Cl_2 was added DMSO (0.18 mL, 2.6 mmol). The solution was maintained at −78 °C for 10 min whereupon a solution of **13** (0.30 g, 0.86 mmol) in CH_2Cl_2 (5.0 mL) was added dropwise. The reaction was stirred at −78 °C for 30 min whereupon TEA (0.60 mL, 4.3 mmol) was added. The reaction was warmed to room temperature, diluted with ethyl acetate and washed sequentially with 1 N HCl, saturated $NaHCO_3$, brine, dried ($MgSO_4$), filtered and concentrated. Column chromatography (1:1 hexanes:ethyl acetate) provided 0.24 g (80%) of **3** as a white powder: ^{1}H NMR (400 MHz, DMSO-d_6, reported as a mixture of diastereomers) δ 8.45 and 8.35 (d, J = 5 Hz, 1 H), 7.35−7.32 (m, 5H), 5.04 (ABq, J = 7.9 Hz, 2H), 4.33−3.76 (m, 6H), 1.61−1.39 (m, 3H), 0.88−0.84 (m, 6H); MS(ESI) 349.0 (M + H)$^+$, 371.0 (M + Na)$^+$. Anal. ($C_{18}H_{24}N_2O_5$) C, H, N, O.

Quinoline-2-carboxylic Acid [(*S*)-1-((3*R*,*S*),(4*R*,*S*)-4-Hydroxytetrahydrofuran-3-ylcarbamoyl)-3-methylbutyl]-amide (15). To a solution of **13** (1.0 g, 2.86 mmol) in methanol (25 mL) was added 10% Pd/C (0.50 g). A balloon of hydrogen gas was attached and the reaction was stirred rapidly for 1 h whereupon it was filtered through a pad of Celite and concentrated to provide 0.6 g (97%) of (*S*)-2-amino-4-methylpentanoic acid ((4*R*,*S*),(3*R*,*S*)-4-hydroxytetrahydrofuran-3-yl)-amide as a clear, light green oil. This material was of sufficient purity to use in the following procedure with no further purification: ^{1}H NMR (400 MHz, $CDCl_3$, reported as a mixture of diastereomers) δ 7.66 (br s, 1H), 4.19−3.99 (m, 4H), 3.68 (m, 2H), 3.85 (m, 1H), 2.65 (br s, 3H), 1.65 (m, 2H), 1.31 (m, 1H), 0.94−0.89 (m, 6H): MS(ESI); 216.8 (M + H)$^+$.

To a solution of (*S*)-2-amino-4-methylpentanoic acid ((4*R*,*S*),-(3*R*,*S*)-4-hydroxytetrahydrofuran-3-yl)amide (0.50 g, 2.31 mmol) in CH_2Cl_2 (5.0 mL) were added quinoline-2-carboxylic acid (0.4 g, 2.31 mmol) and EDC (0.48 g, 2.54 mmol). The reaction was maintained at room temperature for approximately 2 h whereupon it was concentrated. The residue was diluted with ethyl acetate and washed with water, saturated $NaHCO_3$, brine, dried ($MgSO_4$) filtered and concentrated. Column chromatography (3:1 ethyl acetate:hexanes) of the residue provided 0.45 g (52%) of **15** as an off-white solid: ^{1}H NMR (400 MHz, $CDCl_3$, reported as a mixture of diastereomers) δ 8.64−7.31 (m, 7H), 4.72 (m, 1H), 4.36−3.62 (m, 8H), 1.90−1.66 (m, 3H), 0.96−0.83 (m, 6H); MS(ESI) 372 (M + H)$^+$. Anal. ($C_{20}H_{25}N_3O_4$·$55H_2O$) C, H, N.

Quinoline-2-carboxylic Acid [(*S*)-1-((3*R*,*S*)-4-Oxotetrahydrofuran-3-ylcarbamoyl)-3-methylbutyl]amide (16). To a solution of **15** (0.2 g, 0.54 mmol) in DMSO (10 mL) were added sulfur trioxide−pyridine complex (0.26 g, 1.62 mmol) and TEA (0.45 mL, 3.24 mmol). The reaction was maintained at room temperature for 2 h whereupon it was diluted with ethyl acetate and washed with water, saturated $NaHCO_3$, brine, dried ($MgSO_4$), filtered and concentrated. Column chromatography (1:1 ethyl acetate:hexanes) of the residue provided 0.14 g (70%) of ketone **16** as a white powder: ^{1}H NMR (400 MHz, $CDCl_3$, reported as a mixture of diastereomers) δ 8.55 (m, 1H), 8.27−8.10 (m, 3H), 7.84−7.58 (m, 3H), 7.26 (br s, 1H), 4.78−4.75 (m, 1H), 4.62−4.56 (m, 1H), 4.29−43.86 (m, 4H), 1.92−1.74 (m, 3H), 0.99−0.95 (m, 6H); MS(ESI) 370 (M + H)$^+$. Anal. ($C_{20}H_{23}N_3O_4$) C, H, N.

(3*R*,*S*),(4*R*,*S*)-4-Aminotetrahydropyran-3-ol (12). To a solution of the epoxide **10** (1.0 g, mmol) in methanol (40 mL) and water (5 mL) were added NH_4Cl (1.12 g, mmol) and NaN_3 (3.25 g). The reaction was heated to 78 °C until complete consumption of the starting material was observed by TLC analysis. The mixture was concentrated in vacuo to approximately 1/3 the original volume. The mixture was then diluted with ether and washed with saturated $NaHCO_3$, brine, dried ($MgSO_4$), filtered and concentrated to provide (3*R*,*S*),-(4*R*,*S*)-4-azidotetrahydropyran-3-ol which was of sufficient purity to carry onto the following step with no further purification: ^{1}H NMR (400 MHz, $CDCl_3$) δ 3.96 (m, 2H), 3.57 (m, 1H), 3.46 (m, 2H), 3.22 (m,1H) 2.03 (m, 1H), 1.70 (m, 1H).

To a solution of (3*R*,*S*),(4*R*,*S*)-4-azidotetrahydropyran-3-ol (0.20 g, 1.4 mmol) in methanol (3 mL) was added 10% Pd/C (0.1 g). The reaction was stirred rapidly under an atmosphere of hydrogen overnight whereupon it was filtered through a pad of Celite. The filtrate was concentrated to provide the amino alcohol **12**: ^{1}H NMR (400 MHz, $CDCl_3$) δ 3.90 (m, 2H), 3.29 (m, 2H), 3.08 (m, 1H), 2.66, 1H); MS(ESI) 117.8 (M + H)$^+$.

[(*S*)-1-((4*R*,*S*)-3-Oxotetrahydropyran-4-ylcarbamoyl)-3-methylbutyl]carbamic Acid Benzyl Ester (4). To a solution of **12** (0.094 g, 0.8 mmol) in CH_2Cl_2 (10 mL) were added Cbz-leucine (0.21 g, 0.8 mmol) and EDC (0.15 g, 0.85 mmol). The reaction was maintained at room temperature overnight whereupon it was concentrated and the residue chromatographed (100% ethyl acetate) to provide 0.13 g of the alcohol **14**: ^{1}H NMR (400 MHz, $CDCl_3$, reported as a mixture of diastereomers) δ 7.29−7.24 (m, 5H), 6.97−6.84 (m, 1H), 5.81−5.60 (m, 1H), 5.08−4.97 (m, 2H), 4.20−3.83 (m, 4H), 3.42−3.27 (m, 3H), 3.08 (t, 1H), 1.88−1.51 (m, 5H), 0.90−0.86 (m, 6H); MS(ESI) 365.0 (M + H)$^+$, 387.0 (M + Na)$^+$.

To a solution of the alcohol **14** (0.07 g, 0.02 mmol) in DMSO (1.5 mL) were added TEA (0.17 mL, 0.012 mmol) and sulfur trioxide−pyridine complex (0.09 g, 0.06 mmol). The reaction was maintained at room temperature for 2 h whereupon it was diluted with ethyl acetate and washed with saturated $NaHCO_3$, brine, dried ($MgSO_4$), filtered and concentrated to provide ketone **4** as a mixture of diastereomers: ^{1}H NMR (400 MHz, DMSO-d_6, reported as a mixture of diastereomers) δ 8.15 (d, 1H), 7.39−7.29 (m, 5H),5.02 (d, 2H), 4.63 (m, 1H), 4.14−4.10 (m, 2H), 3.97−3.83 (m, 3H), 2.10 (m, 1H), 1.61 (m, 1H), 1.45 (m, 1H), 0.95 (m, 6H); MS(ESI) 363.0 (M + H)$^+$.

[(*S*)-1-((3*R*,*S*),(4*R*,*S*)-4-Hydroxypyrrolidin-3-ylcarbamoyl)-3-methylbutyl]carbamic Acid Benzyl Ester Hydrochloride (19). To a solution of **17** (0.20 g, 1.14 mmol) in CH_2Cl_2 (5.0 mL) were added Cbz-leucine (0.30 g, 1.14 mmol), HOBt (0.15 g, 1.14 mmol) and EDC (0.26 g, 1.37 mmol). The reaction was allowed to stir until complete by TLC analysis whereupon it was diluted with EtOAc and washed sequentially with pH 4 buffer, saturated K_2CO_3, water and brine. The organic layer was dried ($MgSO_4$), filtered and concentrated. Column chromatography of the residue (3:1 EtOAc:hexanes)

provided 0.32 g (62%) of (3*R*,*S*)-((*S*)-2-benzyloxycarbonylamino-4-methylpentanoylamino)-(4*R*,*S*)-4-hydroxypyrrolidine-1-carboxylic acid *tert*-butyl ester: ^{1}H NMR (400 MHz, DMSO-d_6, reported as a mixture of diastereomers) δ 8.11 (m, 1H), 7.44−7.37 (m, 5H), 5.29 (br s, 1H), 5.01 (app s, 2H), 3.97−3.87 (m, 3H), 3.48−3.11 (m, 6H), 1.56 (m, 1H), 1.40 (s, 9H), 0.86−0.83 (m, 6H); MS(ESI) 450.3 $(M + H)^+$, 472.2 $(M + Na)^+$. Anal. ($C_{23}H_{35}N_3O_6$) C, H, N.

To a solution of (3*R*,*S*)-((*S*)-2-benzyloxycarbonylamino-4-methylpentanoylamino)-(4*R*,*S*)-4-hydroxypyrrolidine-1-carboxylic acid *tert*-butyl ester (0.31 g, 0.69 mmol) in dry EtOAc (5.0 mL) was bubbled HCl gas for approximately 5 min. The reaction was stirred until TLC analysis indicated the complete consumption of the starting material. The reaction was then concentrated in vacuo to provide 0.25 g (94%) of **19** as a white solid: ^{1}H NMR (400 MHz, DMSO-d_6, reported as a mixture of diastereomers) δ 8.39 (m, 1H), 7.46 (m, 1H), 7.35 (m, 5H), 5.77 (br s, 1H), 5.01 (m, 2H), 4.16−3.95 (m, 3H), 3.49−3.23 (m, 3H), 3.03 (m, 2H), 1.63−1.45 (m, 3H), 0.89−0.83 (m, 6H); MS(ESI) 350.3 $(M + H)^+$. Anal. ($C_{18}H_{27}N_3O_4$) C, H, N, O.

[(*S*)-1-((3*R*,*S*),(4*R*,*S*)-4-Hydroxypiperidin-3-ylcarbamoyl)-3-methylbutyl]carbamic Acid Benzyl Ester (20). To a solution of **18** (1.0 g, 4.62 mmol) in CH_2Cl_2 were added Cbz-leucine (1.22 g, 4.62 mmol), EDC (1.07 g, 5.58 mmol) and HOBt (0.62 g, 4.62 mmol). The reaction was allowed to stir until complete as indicated by TLC analysis. The reaction was concentrated and the residue dissolved in ethyl acetate, washed with 1 N HCl, saturated $NaHCO_3$, brine, dried, filtered and concentrated. Column chromatography (1:1 hexanes: EtOAc) of the residue provided 0.88 g (42%) of (4*R*,*S*)-((*S*)-2-benzyloxycarbonylamino-4-methylpentanoylamino)-(3*R*,*S*)-hydroxypiperidine-1-carboxylic acid *tert*-butyl ester: ^{1}H NMR (400 MHz, DMSO-d_6, reported as a mixture of diastereomers) δ 7.82−7.72 (m, 1H), 7.33 (m, 5H), 4.99 (m, 2H), 4.90 (m, 1H), 4.02−3.51 (m, 4H), 3.49−3.31−3.25 (m, 1H), 2.66 (br s, 1H), 1.71−1.58 (m, 2H), 1.48−1.36 (m, 2H), 1.37 (s, 9H), 0.86−0.82 (m, 6H); MS(ESI) 464.4 $(M + H)^+$, 486.2 (M + Na). Anal. ($C_{24}H_{37}N_3O_6$) C, H, N.

To a solution of (4*R*,*S*)-((*S*)-2-benzyloxycarbonylamino-4-methylpentanoylamino)-(3*R*,*S*)-hydroxypiperidine-1-carboxylic acid *tert*-butyl ester (0.88 g, 1.96 mmol) in dry EtOAc (10 mL) was bubbled HCl gas for approximately 5 min. The reaction was stirred until TLC analysis indicated complete consumption of the starting material. The reaction was then concentrated in vacuo to give 0.74 g (98%) of **20** as a white powder which was of sufficient purity to carry on to the next step with no further characterization: MS(ESI) 364.3 $(M + H)^+$.

[(*S*)-1-((3*R*,*S*)-1-Acetyl-4-oxopyrrolidin-3-ylcarbamoyl)-3-methylbutyl]carbamic Acid Benzyl Ester (22). To a solution of **19** (0.20 g, 0.57 mmol) in CH_2Cl_2 were added EDC (0.12 g, 0.57 mmol), HOBt (0.077 g, 0.57 mmol), TEA (0.14 g, 1.43 mmol) and acetic acid (0.034 g, 0.57 mmol). The reaction was stirred until complete as indicated by TLC analysis whereupon it was concentrated, the residue dissolved in EtOAc and washed with 0.5 N HCl, saturated $NaHCO_3$, brine, dried ($MgSO_4$), filtered and concentrated. Column chromatography (10% CH_3OH:CH_2Cl_2) of the residue provided 0.096 g (57%) of [(*S*)-1-((3*R*,*S*),(4*R*,*S*)-1-acetyl-4-hydroxypyrrolidin-3-ylcarbamoyl)-3-methylbutyl]carbamic acid benzyl ester as an off-white powder: MS(ESI) 392.2 $(M + H)^+$. Anal. ($C_{20}H_{29}N_3O_5 \cdot 0.1H_2O$) C, H, N, O.

To a −78 °C solution of oxalyl choride (0.01 mL, 0.11 m mol) in CH_2Cl_2 (0.3 mL) was added DMSO (0.016 mL, 0.23 mmol) in CH_2Cl_2 (0.05 mL). The reaction was maintained at −78 °C for approximately 10 min whereupon a solution of [(*S*)-1-((3*R*,*S*),(4*R*,*S*)-1-acetyl-4-hydroxypyrrolidin-3-ylcarbamoyl)-3-methylbutyl]carbamic acid benzyl ester (0.04 g, 0.10 mmol) in CH_2Cl_2 (0.10 mL) was added. The reaction was maintained at −78 °C for another 20 min whereupon TEA (0.07 mL) was added. The mixture was warmed to 0 °C then diluted with EtOAc and washed with saturated $NaHCO_3$, brine, dried ($MgSO_4$) filtered and concentrated. Column chromatography (3% CH_3OH:CH_2Cl_2) provided 0.015 g (35%) of **22** as an off white powder: ^{1}H NMR (400 MHz, $CDCl_3$, reported as a 1:1 mixture of diastereomers) δ 7.22 (m, 5H), 6.15−5.87 (m, 1H), 4.97 (m, 2H), 4.19−3.16 (m, 7H), 1.99−1.81 (m, 3H), 1.56−1.46 (m, 3H), 1.19−1.31.09 (m, 2H), 0.89−0.83 (m, 6H); MS-(ESI) 390.1 $(M + H)^+$, 779.3 $(2M + H)^+$. Anal. ($C_{20}H_{27}N_3O_5 \cdot 0.25$EtOAc) C, H, N, O.

((*S*)-1-{[(3*R*,*S*)-((*S*)-2-Benzyloxycarbonylamino-4-methylpentanoylamino)-4-oxopyrrolidin-1-yl]methanoyl}-3-methylbutyl)carbamic Acid Benzyl Ester (24). To a solution of **19** (0.25 g, 0.64 mmol) in CH_2Cl_2 (10 mL) were added Cbz-leucine (0.17 g, 0.64 mmol), HOBt (0.08 g, 0.64 mmol), NMM (0.300 mL) and EDC (0.15 g, 0.77 mmol). The reaction was allowed to stir at room temperature for 2 h whereupon it was diluted with ethyl acetate and washed sequentially with 1 N HCl, saturated K_2CO_3, water and brine. The organic layer was dried ($MgSO_4$), filtered and concentrated. Column chromatography of the residue (3:1 EtOAc: hexanes) gave 0.1 g (26%) of ((*S*)-1-{1-[(3*R*,*S*)-((*S*)-2-benzyloxycarbonylamino-4-methylpentanoylamino)-(4*R*,*S*)-hydroxypyrrolidin-1-yl]methanoyl}-3-methylbutyl)carbamic acid benzyl ester: ^{1}H NMR (400 MHz, $CDCl_3$; reported as a mixture of diastereomers) δ 7.31−7.26 (m, 12H), 5.76−5.44 (m, 3H), 5.13−4.90 (m, 5H), 4.37−4.12 (m, 8H), 1.69−1.46 (m, 6H), 0.96−0.87 (m, 12H); MS(ESI) 597.1 $(M + H)^+$, 619.1 $(M + Na)^+$. Anal. ($C_{32}H_{46}N_4O_7 \cdot 0.5H_2O$) C, H, N, O.

To a 0 °C solution of of ((*S*)-1-{1-[(3*R*,*S*)-((*S*)-2-benzyloxycarbonylamino-4-methylpentanoylamino)-(4*R*,*S*)-hydroxypyrrolidin-1-yl]methanoyl}-3-methylbutyl)carbamic acid benzyl ester (0.10 g, 0.17 mmol) in acetone (5.0 mL) was added Jone's reagent dropwise until the brown color persisted. The reaction was allowed to warm to room temperature and stirred approximately 48 h whereupon it was quenched with 2-propanol, diluted with EtOAc and washed sequentially with saturated K_2CO_3, water and brine. The organic layer was dried ($MgSO_4$), filtered and concentrated. Column chromatography of the residue (3:1 EtOAc:hexanes) gave 0.03 g of **24** as a white powder: MS(ESI) 595.1 $(M + H)^+$, 617.0 $(M + Na)^+$. Anal. ($C_{32}H_{44}N_4O_7$) C, H, N, O.

((*S*)-1-{[(3*R*,*S*)-((*S*)-2-(Benzyloxycarbonylmethylamino)-4-methylpentanoylamino)-4-oxopyrrolidin-1-yl]methanoyl}-3-methylbutyl)carbamic Acid Benzyl Ester (25). To a solution of **19** (0.1 g, 0.26 mmol) in CH_2Cl_2 (5.0 mL) were added *N*-methyl-Cbz-leucine (0.07 g, 0.26 mmol), HOBt (0.03 g, 0.64 mmol), NMM (0.30 mL) and EDC (0.06 g, 0.31 mmol). The reaction was allowed to stir at room temperature for 2 h whereupon it was diluted with ethyl acetate and washed sequentially with 1 N HCl, saturated K_2CO_3, water and brine. The organic layer was dried ($MgSO_4$), filtered and concentrated. Column chromatography of the residue (3:1 EtOAc:hexanes) gave 0.13 g (82%) of ((*S*)-1-{[(3*R*,*S*)-((*S*)-2-(benzyloxycarbonylmethylamino)-4-methylpentanoylamino)-(4*R*,*S*)-hydroxypyrrolidin-1-yl]methanoyl}-3-methylbutyl)carbamic acid benzyl ester: ^{1}H NMR (400 MHz, $CDCl_3$; reported as a mixture of diastereomers) δ 7.33−7.26 (m, 10H), 5.13−4.99 (m, 4H), 4.31−3.25 (m, 7H), 3.03−2.84 (m, 4H), 1.79−1.40 (m, 5H), 0.93−0.83 (m, 12H); MS(ESI) 611.3 $(M + H)^+$, 632.9 $(M + Na)^+$.

To a −78 °C solution of oxalyl chloride (0.013 mL, 0.13 mmol) in CH_2Cl_2 (5.0 mL) was added DMSO (0.018 mL, 0.26 mmol). The reaction was maintained at −78 °C for 10 min whereupon a solution of ((*S*)-1-{[(3*R*,*S*)-((*S*)-2-(benzyloxycarbonylmethylamino)-4-methylpentanoylamino)-(4*R*,*S*)-hydroxypyrrolidin-1-yl]methanoyl}-3-methylbutyl)carbamic acid benzyl ester (0.075 g, 0.12 mmol) in CH_2Cl_2 (2.0 mL) was added in a dropwise fashion. The reaction was maintained at −78 °C for 30 min whereupon TEA (0.083 mL, 0.6 mmol) was added. The reaction was warmed to room temperature, diluted with ethyl acetate and washed with 1 N HCl, saturated K_2CO_3, water and brine. The organic layer was dried ($MgSO_4$), filtered and concentrated. Column chromatography (2:1 ethyl acetate: hexanes) of the residue provided 0.04 g (55%) of **25** as a white solid: ^{1}H NMR (400 MHz, $CDCl_3$, reported as a mixture of diastereomers) δ 7.35−7.25 (m, 10H), 5.15−5.10

(m, 6H), 4.95−3.40 (m, 6H), 2.93−2.83 (m, 3H), 1.67−1.36 (m, 6H), 0.97−0.91 (m, 12H); MS(ESI) 609.1 $(M + H)^+$, 630.8 $(M + Na)^+$.

((*S*)-1-{[(4*R*,*S*)-((*S*)-2-Benzyloxycarbonylamino-4-methylpentanoylamino)-3-oxopiperidin-1-yl]methanoyl}-3-methylbutyl)carbamic Acid Benzyl Ester (27). To a solution of **20** (0.15 g, 0.43 mmol) in CH_2Cl_2 were added Cbz-leucine (0.11 g, 0.43 mmol), EDC (0.1 g, 0.52 mmol), HOBt (0.058 g, 0.43 mmol) and NMM (0.14 mL, 1.28 mmol). The reaction was stirred until complete as indicated by TLC analysis. Workup and column chromatography (2:1 EtOAc: hexanes) gave 0.22 g (84%) of ((*S*)-1-{[(4*R*,*S*)-((*S*)-2-benzyloxycarbonylamino-4-methylpentanoylamino)-(3*R*,*S*)-hydroxypiperidin-1-yl]methanoyl}-3-methylbutyl)carbamic acid benzyl ester: MS(ESI) 611.2 $(M + H)^+$, 633.2 $(M + Na)^+$. Anal. ($C_{33}H_{46}N_4O_7$) C, H, N, O.

To a −78 °C solution of oxalyl chloride (0.043 mL, 0.49 mmol) in CH_2Cl_2 (5.0 mL) was added DMSO (0.07 mL, 0.98 mmol). The reaction was maintained at −78 °C for 10 min whereupon a solution of ((*S*)-1-{[(4*R*,*S*)-((*S*)-2-benzyloxycarbonylamino-4-methylpentanoylamino)-(3*R*,*S*)-hydroxypiperidin-1-yl]methanoyl}-3-methylbutyl)carbamic acid benzyl ester (0.19 g, 0.32 mmol) in CH_2Cl_2 (3 × 2.0 mL) was added in a dropwise fashion. The reaction was maintained at −78 °C for 30 min whereupon TEA (0.23 mL, 1.63 mmol) was added. The reaction was warmed to room temperature, diluted with ethyl acetate and washed with 1 N HCl, saturated K_2CO_3, water and brine. The organic layer was dried ($MgSO_4$), filtered and concentrated. Column chromatography (2:1 ethyl acetate:hexanes) of the residue provided 0.11 g (54%) of **27** as a white solid: MS(ESI) 611.2 $(M + H)^+$, 633.2 $(M + Na)^+$. Anal. ($C_{33}H_{44}N_4O_7$) C, H, N, O.

[(*S*)-1-(3*RS*,4*RS*)-4-Hydroxy-tetrahydro-furan-3-ylcarbamoyl)-3-methylbutyl]carbamic Acid Benzyl Ester (36). To a solution of *trans*-2-aminocyclopentanol **34** (1.00 g, 6.59 mmol) in CH_2Cl_2 (20 mL) were added Cbz-leucine (1.75 g, 6.59 mmol), EDC (1.23 g, 6.59 mmol) and *N*-methylmorpholine. The reaction was maintained at room temperature overnight whereupon it was concentrated in vacuo and the residue dissolved in ethyl acetate and washed with 1 N HCl, saturated $NaHCO_3$, water and brine. The organic layer was dried ($MgSO_4$), filtered and concentrated. Column chromatography (2:1 ethyl acetate:hexanes provided 1.16 g of **36** as a white solid: ^{1}H NMR (400 MHz, $CDCl_3$, reported as a mixture of diastereomers) δ 7.38−7.32 (m, 5H), 6.41 (br s, 1H), 5.25 (m, 1H), 5.11 (app s, 2H), 4.17 (m, 1H), 3.92 (m, 1H), 3.79 (m, 1H), 3.49 (m, 1H), 2.11−1.53 (m, 8H), 0.95 (m, 6H); MS(ESI) 349.1 $(M + H)^+$.

[(*S*)-1-((*R*,*S*)-2-Oxocyclopentylcarbamoyl)-3-methylbutyl]carbamic Acid Benzyl Ester (8). To a solution of **37** (0.50 g, 1.37 mmol) in DMSO (5.0 mL) was added sulfur trioxide−pyridine complex (0.66 g, 4.13 mmol). The reaction was stirred for approximately 2 h whereupon it was diluted with ethyl acetate and washed with 1 N HCl, water and brine. The organic layer was dried ($MgSO_4$), filtered and concentrated. Column chromatography (1:1 ethyl acetate:hexanes) provided 0.48 g of **8** as a white solid: ^{1}H NMR (400 MHz, $CDCl_3$, reported as a mixture of diastereomers) δ 7.31 (m, 5H), 6.87 (m, 1H), 5.65 (m, 1H), 5.28 (m, 2H), 4.50 (m, 1H), 4.09 (m, 1H), 2.49−1.53 (m, 8H), 0.91 (m, 6H); MS(ESI) 347.3 $(M + H)^+$.

X-ray Crystallography: 1. Crystallization of the Complex of Cathepsin K with Inhibitor 16. Crystals of mature activated cathepsin K complexed with the inhibitor were grown by the vapor diffusion method from a solution of 30% MPD, 0.1 M MES, 0.1 M Tris at pH 7.0. Crystals of the complex are orthorhombic, space group $P2_12_12_1$, with cell constants of a = 38.5 Å, b = 51.3 Å, and c = 104.2 Å. The structure was determined as described described below for the complex of cathepsin K with inhibitor **29** and refined at 2.5 Å. The final R_c was 0.201.

2. Crystallization of the Complex of Cathepsin K with Inhibitor 29. Crystals of mature activated cathepsin K complexed with the inhibitor were grown by the vapor diffusion method from a solution of 18% PEG 8000, 0.06 M sodium acetate at pH 4.5 containing 0.12 M Li_2SO_4. Crystals of the complex are tetragonal, space group $P4_32_12$, with cell constants of a = 57.9 Å and c = 130.3 Å. The structure was determined by molecular replacement with a model consisting of all protein atoms from the previously determined cathepsin K/E-64 complex.[36] The structure was refined at 2.4 Å resolution. The final R_c was 0.218.

3. Crystallization of the Complex of Cathepsin K with Inhibitor 33. Crystals of mature activated cathepsin K complexed with the inhibitor were grown by the vapor diffusion method from a solution of 30% MPD, 0.1 M MES, 0.1 M Tris at pH 7.0. Crystals of the complex are orthorhombic, space group $P2_12_12_1$, with cell constants of a = 38.2 Å, b = 50.6 Å, and c = 102.3 Å. The structure was determined as described above for the complex of cathepsin K with inhibitor **29** and refined at 1.9 Å. The final R_c was 0.253.

Mass Spectral Analysis of Cathepsin K/Inhibitor Complexes. The inhibitors were prepared at a 5-fold molar concentration to the enzyme in water (Milli-Q 18 MΩ) with a 20% final volume of DMSO making sure that the inhibitor was completely dissolved. Human cathepsin K was provided in buffer (100 mM sodium acetate, 100 mM NaCl, 2 mM L-cysteine, pH 5.5). The enzyme, 1 nmol, was mixed with inhibitor solution 1:1 in a 0.65-mL plastic centrifuge tube, vortexed and a minimum of 120-min incubation time was allowed before analysis by LC−MS. The entire reaction mixture was injected onto the peptide trap. The trap was washed with 1 mL of water (Milli-Q 18 MΩ) manually before being back-eluted onto the analytical column.

Supporting Information Available: Lineweaver−Burk plots for **3** and **24**. This material is available free of charge via the Internet at http://pubs.acs.org.

References

(1) (a) McKerrow, J. H., James, M. N. G., Eds. Cysteine proteases: evolution, function and inhibitor design. *Perspect. Drug Disovery Des*. **1996**, *6*, 1−125. (b) Chapman, H. A.; Riese, R. J.; Shi, G.-P. Emerging roles for cysteine proteases in human biology. *Annu. Rev. Physiol*. **1997**, *59*, 63−88.

(2) Krantz, A. Proteinases in inflammation. *Annu. Rep. Med. Chem*. **1993**, *28*, 187.

(3) (a) Frosch, B. A.; Sloane, B. F. The role of proteolytic enzymes in brain tumor infiltration. *Brain Tumor Invasion* **1998**, 275−300. (b) Elliott, E. E.; Sloane, B. F.; The cysteine protease cathepsin B in cancer. *Perspect. Drug Disovery Des*. **1996**, *6*, 12−32.

(4) (a) Cazzulo, J. J.; Stoka, V.; Turk, V. Cruzipain, the major cysteine proteinase from the protazoan parasite *Trypanosoma cruzi*. *J. Biol. Chem*. **1997**, *378*, 1−10. (b) McKerrow, J. H. Cysteine proteases of parasites: a remarkable diversity of function. *Perspect. Drug Discovery Des*. **1995**, *2*, 437. (c) McKerrow, J. H.; Sun, E. Rosenthal, P. J.; Bouvier, J. The proteases and pathogenicity of parasitic protazoa. *Annu. Rev. Microbiol*. **1993**, *47*, 821−853. (d) McKerrow, J. H. Development of cysteine protease inhibitors as chemotherepy for parasitic diseases: insights on safety, target validation, and mechanism of action. *Int. J. Parasitol*. **1999**, *29*, 833−837.

(5) Gowen, M. Inhibition of cathepsin K−a novel approach to antiresorptive therapy. *Exp. Opin. Invest. Drugs* **1997**, *6*, 1999−2002.

(6) (a) Drake, F. H.; Dodds, R. A.; James, I. A.; Connor, J. R.; Debouck, C.; Richardson, S.; Lee-Rykaczewski, L.; Coleman, L.; Riemann, D.; Barthlow, R.; Hastings, G.; Gowen, M. Cathepsin K, but not cathepsins B, L or S is abundantly expressed in human osteoclasts. *J. Biol. Chem*. **1996**, *271*, 12511−12516. (b) Brömme, D.; Okamoto, K. Human cathepsin O2, a novel cysteine protease highly expressed in osteoclastomas and ovary. Molecular cloning, sequencing and tissue distribution. *Biol. Chem. Hoppe-Seyler* **1995**, *376*, 379−384. (c) Shi, G.-P.; Chapman, H. A.; Bhairi, S. M.; DeLeeuw, C.; Reddy, V. Y.; Weiss, S. J. Molecular cloning of human cathepsin O, a novel endoproteinase and homologue of rabbit OC2. *FEBS Lett*. **1995**, *357*, 129−134. (d) Littlewood-Evans, A.; Kokubo, T.; Ishibashi, O.; Inaoka, T.; Wlodarski, B.; Gallagher, J. A.; Bilbe, G. Localization of cathepsin K in human osteoclasts by *In Situ* hybridization and immunohistochemistry. *Bone* **1997**, *20*, 81−86. (e) Bossard, M.

J.; Tomaszek, T. A.; Thompson, S. K.; Amegadzie, B. Y.; Hanning, C. R.; Jones, C., Kurdyla, J. T.; McNulty, D. E.; Drake, F. H.; Gowen, M.; Levy, M. A. Proteolytic activity of human osteoclast cathepsin K. Expression, activation and substrate identification. *J. Biol. Chem*. **1996**, *271*, 12517−12524.

(7) (a) Gelb, B. D.; Moissoglu, K.; Zhang, J.; Martignetti, J. A.; Brömme, D.; Desnick, R. J. Cathepsin K; isolation and characterization of the murine cDNA and genomic sequence, the homologue of the human pycnodysostosis Gene. *Biochem Mol. Med*. **1996**, *59*, 200−206. (b) Johnson, M. R.; Polymeropoulos, M. H.; Vos, H. L.; Oritz de Luna, R. I.; Francomano, C. A. A nonsense mutation in the cathepsin K gene observed in a family with pycnodysostosis. *Genome Res*. **1996**, *6*, 1050−1055. (c) Gelb, B. D.; Shi, G.-P.; Chapman, H. A.; Desnick, R. J. Pycnodysostosis, a lysosomal disease caused by cathepsin K deficiency. *Science* **1996**, *273*, 1236−1238.

(8) Inui, T.; Ishibashi, O.; Inaoka, T.; Origane, Y.; Kumegawa, M.; Kokubo, T.; Yamaura, T. Cathepsin K antisense oligodeoxynucleotide inhibits osteoclastic bone resorption. *J. Biol. Chem*. **1997**, *272*, 8109−8112.

(9) (a) Saftig, P.; Hunziker, E.; Wehmeyer, O.; Jones, S.; Boyde, A.; Rommerskirch, W.; Detlev, J. D.; Schu, P.; von Figura, K. Impaired osteoclastic bone resorption leads to osteopetrosis in cathepsin K deficient mice. *Proc. Natl. Acad. Sci. U.S.A*. **1998**, *95*, 13453−13458. (b) Gowen, M.; Lazner, F.; Dodds, R.; Kapadia, R.; Field, J.; Tavaria, M.; Bertoncello, I.; Drake, F.; Zavarselk, S.; Tellis, I.; Hertzog, P.; Debouck, C.; Kola, I. Cathepsin K knockout mice develop osteopetrosis due to a deficit in matrix degradation but not demineralization. *J. Bone Miner. Res*. **1999**, *14*, 1654−1663.

(10) Reviews on cysteine protease inhibition: (a) Rasnick, D. Small synthetic inhibitors of cysteine proteases. *Perspect. Drug Discovery Des*. **1996**, *6*, 47−63. (b) Otto, H.-H.; Schirmeister, T. Cysteine proteases and their inhibitors. *Chem. Rev*. **1997**, *97*, 133−171. (c) Leung, D.; Abbenante, G.; Fairle, D. P. Protease inhibitors: current status and future prospects. *J. Med. Chem*. **2000**, *43*, 305−341.

(11) Matsumoto, K.; Mizoue, K.; Kitamura, K.; Tse, W.-C.; Huber, C. P.; Ishida, T. Structural basis of the inhibition of cysteine proteases by E-64 and its derivatives. *Biopolymers* **1999**, *51*, 99−107.

(12) (a) Smith, R. A.; Copp, L. J.; Coles, P. J.; Pauls, H. W.; Robinson, V. J.; Spencer, R. W.; Heard, S. B.; Krantz, A. New inhibitors of cysteine proteases. Peptidyl acyloxymethyl ketones and the quiescent nucleofuge strategy. *J. Am. Chem. Soc*. **1988**, *110*, 4429−04431. (b) Krantz, A. Some thoughts on enzyme inhibition and the quiescent affinity label concept. *Adv. Med. Chem*. **1992**, *1*, 235−261. (c) Krantz, A. Peptidyl(acyloxy)methanes as quiescent affinity labels for cysteine proteases. *Methods Enzymol*. **1994**, *244*, 656−671.

(13) (a) Palmer, J. T.; Rasnick, D.; Klaus, J. L.; Brömme, D. Vinyl sulfones as mechanism-based cysteine protease inhibitors. *J. Med. Chem*. **1995**, *38*, 3193−3196. (b) Brömme, D.; Klaus, J. L.; Okamoto, K.; Rasnick, D.; Palmer, J. T. Peptidyl vinyl sulphones: a new class of potent and selective cysteine protease inhibitors. *Biochem. J*. **1996**, *315*, 85−89. (c) McGrath, M. E.; Klaus, J. L.; Barnes, M. G.; Brömme, D. Crystal structure of human cathepsin K complexed with a potent inhibitor. *Nat. Struct. Biol*. **1997**, *4*, 105−109.

(14) (a) Hanzlik, R. P.; Thompson, S. A. Vinylogous amino acid esters: a new class of inactivators for thiol proteases. *J. Med. Chem*. **1984**, *27*, 711−712. (b) Matthews, D. A.; Dragovich, P. S.; Webber, S. E.; Fuhrman, S. A.; Patick, A. K.; Kalman, L. S.; Hendrickson, T. F.; Love, R. A.; Pins, T. J.; Marakovits, J. T.; Zhou, R.; Tikhe, J.; Ford, C. E.; Meador, J. W.; Ferre, R. A.; Brown, E. L.; Binford, S. L.; Brothers, M. A.; DeLisle, D. M.; Worland, S. T. Structure-assisted design of mechanism-based irreversible inhibitors of human rhinovirus 3C protease with potent antiviral activity against multiple rhinovirus serotypes. *Proc. Natl. Acad. Sci. U.S.A.*. **1999**, *96*, 11000−11007 and references therein.

(15) Recent examples include: (a) Votta, B. J.; Levy, M. A.; Badger, A.; Bradbeer, J.; Dodds, R. A.; James, I. E.; Thompson, S.; Bossard, M. J.; Carr, T.; Conner, J. R.; Tomaszek, T. A.; Szewczuk, L.; Drake, F. H.; Veber, D. F.; Gowen, M. Peptide aldehyde inhibitors of cathepsin K inhibit bone resorption both in vitro and in vivo. *J. Bone Mineral Res*. **1997**, *12*, 1396−1406. (b) Yasuma, T.; Oi, S.; Choh, N.; Nomura, T.; Furuyama, N.; Nishimura, A.; Fujisawa, Y.; Sohda, T. Synthesis of peptide aldehyde derivatives as selective inhibitors of human cathepsin L and their inhibitory effect on bone resorption. *J. Med. Chem*. **1998**, *41*, 4301−4308. (c) Karanewsky, D. S.; Bai, X.; Linton, S. D.; Krebs, J. F.; Wu, J.; Pham, B.; Tomaselli, K. J. Conformationally constrained inhibitors of caspase-1 (interleukin-1β converting enzyme) and of the human CED-3 homologue caspase-3 (CPP32, apopain). *Bioorg. Med. Chem. Lett*. **1998**, *8*, 2757−2762.

(16) (a) Ando, R.; Morinaka, Y. A new class of proteinase inhibitor. Cyclopropenone-containing inhibitor of papain. *J. Am. Chem. Soc*. **1993**, *115*, 1174−1175. (b) Ando, R.; Sakaki, T.; Morinaka, Y.; Takahashi, C.; Tamao, Y.; Yoshii, N.; Katayama, S.; Saito, K.; Tokuyama, H.; Isaka, M.; Nakamura, E. Cyclopropeneone-containing cysteine proteinase inhibitors. Synthesis and enzyme inhibitory activities. *Bioorg. Med. Chem*. **1999**, *7*, 571−579.

(17) (a) Moon, J. B.; Coleman, R. S.; Hanzlik, R. P. Reversible covalent inhibition of papain by a peptide nitrile. ^{13}C NMR evidence for a thioimidate ester adduct. *J. Am. Chem. Soc*. **1986**, *108*, 1350−1351. (b) Brisson, J.-R.; Carey, P. R.; Storer, A. C.; Benzoylamidoacetonitrile is bound as a thioimidate in the active site of papain. *J. Biol. Chem*. **1986**, *261*, 9087−9089. (c) Liang, T.-C.; Abeles, R. H. Inhibition of papain by nitriles: mechanistic studies using NMR and kinetic measurements. *Arch. Biochem. Biophys*. **1987**, *252*, 626−634.

(18) (a) Hu, L.-Y.; Abeles, R. H. Inhibition of cathepsin B and papain by peptidyl α-keto esters, α-keto amides α-diketones and α-keto acids. *Arch. Biochem. Biophys*. **1990**, *281*, 271−274. (b) Li, Z.; Patil, G. S.; Golubski, Z. E.; Hori, H.; Tehrani, K.; Foreman, J. E.; Eveleth, D. D.; Bartus, R. T.; Powers, J. C. Peptide α-keto ester, α-keto amide, and α-keto acid inhibitors of calpains and other cysteine proteases. *J. Med. Chem*. **1993**, *36*, 3472−3480. (c) Harbeson, S. L.; Abelleira, S. M.; Akiyama, A.; Barrett III, R.; Carroll R. M. Straub, J. A. Tkacz, J. N.; Wu, C.; Musso, G. F. Stereospecific synthesis of peptidyl α-keto amides as inhibitors of calpain. *J. Med. Chem*. **1994**, *37*, 2918−2929.

(19) (a) Majalli, A. M. M.; Chapman, K. T.; MacCoss, M.; Thornberry, N. A.; Peterson, E. P. Activated ketones as potent reversible inhibitors of interleukin-1β converting enzyme. *Bioorg. Med. Chem. Lett*. **1994**, *4*, 1965−1968. (b) Yamashita, D. S.; Smith, W. W.; Zhao, B.; Janson, C. A.; Tomaszek, T. A.; Bossard, M. A.; Levy, M. A.; Oh, H.-J.; Carr, T. J.; Thompson, S. T.; Ijames, C. F.; Carr, S. A.; McQueney, M.; D′Alessio, K. J.; Amegadzie, B. Y.; Hanning, C. R.; Abdel-Meguid, S.; DesJarlais, R. L.; Gleason, J. G.; Veber, D. F. Structure and design of potent and selective cathepsin K inhibitors. *J. Am. Chem. Soc*. **1997**, *119*, 11351−11352. (c) DesJarlais, R. L.; Yamashita, D. S.; Oh, H.-J.; Uzinskas, I. N.; Erhard, K. F.; Allen, A. C.; Haltwanger, R. C.; Zhao, B.; Smith, W. W.; Abdel-Meguid, S. S.; D'Allesio, K.; Janson, C. A.; McQueney, M. S.; Tomaszek, T. A.; Levy, M. A.; Veber, D. F. Use of X-ray cocrystal structures and molecular modeling to design potent and selective non-peptide inhibitors of cathepsin K. *J. Am. Chem. Soc*. **1998**, *35*, 9114−9115.

(20) Amos, H. E.; Park, B. K. In *Immunotoxicology and Immunopharmacology*; Raven Press: New York, 1985; pp 207−228.

(21) Marquis, R. W.; Ru, Y.; Yamashita, D. S.; Oh, H.-J.; Yen, J.; Thompson, S. K.; Carr, T. J.; Levy, M. A.; Tomaszek, T. A.; Ijames, C. F.; Smith, W. W.; Zhao, B.; Janson, C. A.; Abdel-Meguid, S. S.; D'Alessio, K. J.; McQueney, M. S.; Veber, D. F. Potent dipeptidyl ketone inhibitors of the cysteine protease cathepsin K. *Bioorg. Med. Chem*. **1999**, *7*, 581−588.

(22) (a) Jones, D. M.; Atrash, B.; Teger-Nilsson, A.-C.; Gyzander, E.; Deinum, J.; Szelke, M.; Design and synthesis of thrombin inhibitors. *Lett. Pept. Sci*. **1995**, *2*, 147−154. (b) Jones, M. D.; Atrash, B.; Teger-Nilsson, A. C.; Gyzander, E.; Deinum, J.; Szelke, M. Inhibitors of thrombin containing arginine ketone derivatives. *Proc. Eur. Pept. Symp. 23rd* **1995**, 899−900. (c) Jones, D. M.; Atrash, B.; Ryder, H.; Teger-Nilsson, A.-C.; Gyzander, E.; Szelke, M. Thrombin inhibitors based on ketone derivatives of arginine and lysine. *J. Enzyme Inhib*. **1995**, *9*, 43−60.

(23) The nomenclature of Schecter and Berger: Schecter, I.; Berger, A. On the size of the active site in proteases I. Papain. *Biochem. Biophys. Res. Commun*. **1967**, *27*, 157−162.

(24) The following numbering system has been used:

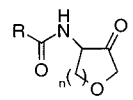

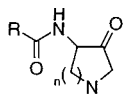

n = 1: 3-amidotetrahydrofuran-4-one n = 1; 3-amido-pyrrolidin-4-one

n = 2: 4-amido-tetrahydropyran-3-one n = 2; 4-amido-piperidin-3-one

(25) Marquis, R. W.; Yamashita, D. S.; Ru, Y.; LoCastro, S. M.; Oh, H.-J.; Erhard, K. F.; DesJarlais, R. L.; Head, M. S.; Smith, W. W.; Zhao, B.; Janson, C. A.; Abdel-Meguid, S. S.; Tomaszek, T. A.; Levy, M. A.; Veber, D. F. Conformationally constrained 1,3-diamino ketones: A series of potent and selective inhibitors of the cysteine protease cathepsin K. *J. Med. Chem*. **1998**, *41*, 3563−3567.

(26) For a discussion regarding the regioselective opening of 3,4-epoxytetrahydropyrans, see: Berti, G.; Catelani, G.; Ferretti, M.; Monti, L. Regio- and stereoselectivity of the three-membered ring opening of 3,4-epoxytetrahydropyrans and of the corresponding epibromonium ions. *Tetrahedron* **1974**, *30*, 4013−4020.

(27) Parikh, J. R.; Doering, v. W. E.; Sulfur trioxide in the oxidation of alcohols by dimethyl sulfoxide. *J. Am. Chem. Soc.* **1967**, *89*, 5505.
(28) Hong, H.; Mendoza, J. S.; Lowden, C. T.; Ballas, L. M.; Janzen, W. P. Synthesis and protein kinase C activities of balanol analogues with modification of the 4-hydroxbenzamido moiety. *Bioorg. Med. Chem.* **1997**, *5*, 1873−1882.
(29) Marquis, R. W.; Veber, D. F.; Ru, R.; LoCastro, S. M. WO9805336.
(30) Inhibitor potencies verses purified recombinant cathepsin K were evaluated according to the procedure of reference 15a. Human liver cathepsins B and L were purchased from Calbiochem. Inhibitors were assayed against recombinant human cathepsin S, human liver cathepsin L and human liver cathepsin B utilizing the following substrates respectively: Cbz-Val-Val-Arg-AMC at 20 μM (K_m = 25 μM), Cbz-Phe-Arg-AMC at 5 μM (K_m = 3 μM), and Cbz-Phe-Arg-AMC at 50 μM (K_m = 140 μM), respectively, in 100 mM acetate, 20 mM cysteine, 5 mM EDTA, pH 5.5 buffer with a final DMSO concentration of 10%.
(31) (a) Abeles, R. H. Enzyme inhibitors: Ground state/transition state analogues. *Drug Dev. Res.* **1987**, *10*, 221−234. (b) Douglas, D. T. Transition-state analogues in drug design. *Chem. Ind. (London)* **1983**, *8*, 311−315. (c) Brodbeck, U. Recent developments in the field of enzyme inhibitors. *Chima* **1980**, *34*, 415−421. (d) Lienhard, G. E. Transition state analogues as enzyme inhibitors. *Annu. Rep. Med. Chem.* **1972**, *7*, 249−258. (e) Radzika, A.; Wolfenden, R. Transition state and multisubstrate analogue inhibitors. *Methods Enzymol.* **1995**, *249*, 284−312
(32) (a) Fenwick, A. E.; Gribble, A. D.; Ife, R. J.; Stevens, N.; Witherington, J. Diastereoselective synthesis, activity and chiral stability of cyclic alkoxy ketone inhibitors of cathepsin K. *Bioorg. Med. Chem Lett.*, submitted for publication. (b) Fenwick, A. E.; Garnier, B.; Gribble, A. D.; Ife, R. J.; Rawlings, A. D.; Witherington, J. Solid-phase synthesis of cyclic alkoxy ketones, inhibitors of the cysteine protease cathepsin K. *Bioorg. Med. Chem. Lett.*, submitted for publication.
(33) Hunter, C. A.; Sanders, J. K. M. The nature of $\pi-\pi$ interactions. *J. Am. Chem. Soc.* **1990**, *112*, 5525−5534.
(34) The utility of the through-space effect for the design of ketone-based cysteine protease inhibitors has been eloquently demonstrated by Seto and co-workers. See: (a) Conroy, J. L.; Sanders, T. C.; Seto, C. T. Using the electrostatic field effect to design a new class of inhibitors for cysteine proteases. *J. Am. Chem. Soc.* **1997**, *119*, 4285−4291. (b) Conroy, J. L.; Abato, P.; Ghosh, M.; Austermuhle, M. I.; Kiefer, M. R.; Seto, C. T. Synthesis of cyclohexanone-based cathepsin B inhibitors that interact with both the S and S′ binding sites. *Tetrahedron Lett.* **1998**, *39*, 8253−8256.
(35) Berman, J.; Halm, K.; Adkinson, K.; Shaffer, J. Simultaneous pharmacokinetic screening of a mixture of compounds in the dog using API LC/MS/MS analysis for increased throughput. *J. Med. Chem.* **1997**, *40*, 827−829.
(36) Zhao, B.; Janson, C. A.; Amegadzie, B. Y.; D'Alessio, K.; Griffin, C.; Hanning, C. R.; Jones, C.; Kurdyla, J.; McQueney, M.; Qiu, X.; Smith, W. W.; Abdel Meguid, S. S. Crystal structure of human osteoclast cathepsin K complex with E-64. *Nat. Struct. Biol.* **1997**, *4*, 109−111.

JM000320T